Draft version July 4, 2012
Preprint typeset using LaTeX style emulateapj v. 11/26/04
gritschneder@ucolick.org

arXiv:1207.0495v1 [astro-ph.SR] 2 Jul 2012

THE ROLE OF θ OPH IN THE FORMATION AND EVOLUTION OF THE PIPE NEBULA - IS STAR FORMATION EVER ISOLATED?

Matthias Gritschneder[1,2] and Douglas N.C. Lin[1,2]
[1]Kavli Institute for Astronomy and Astrophysics, Peking University,Yi He Yuan Lu 5, Hai Dian, 100871 Beijing, China;
[2]Astronomy and Astrophysics Department, University of California, Santa Cruz, CA 95064, USA
Draft version July 4, 2012

ABSTRACT

We propose that the Pipe Nebula is an HII region shell swept up by the B2 IV β Cephei star θ Ophiuchi. After reviewing the morphological evidence by recent observations, we perform a series of analytical calculations. We use realistic HII region parameters derived with the radiative transfer code Cloudy from observed stellar parameters. We are able to show that the current size, mass and pressure of the region can be explained in this scenario. We investigate the configuration today and come to the conclusion that the Pipe Nebula can be best described by a three phase medium in pressure equilibrium. The pressure support is provided by the ionized gas and mediated by an atomic component to confine the cores at the observed current pressure. In the future, star formation in these cores is likely to be either triggered by feedback of the most massive, gravitationally bound cores as soon as they collapse or by the supernova explosion of θ Ophiuchi itself.

Subject headings: HII regions — ISM: clouds — ISM: individual objects: Pipe Nebula — ISM: structure — methods: analytical — methods: numerical—stars: formation

1. INTRODUCTION

The Pipe Nebula, first observed by Onishi et al. (1999) is a nearby molecular cloud region. Due to its relative proximity ($D \approx 130\,\mathrm{pc}$, Lombardi et al. 2006, $D \approx 145\,\mathrm{pc}$, Alves & Franco 2007) it provides an ideal testbed to observe molecular cloud core formation (Lada et al. 2008). The total spatial extend of the Pipe Nebular is roughly $14\,\mathrm{pc} \times 3\,\mathrm{pc}$. The early measurements by Onishi et al. (1999) showed the gaseous component emitting ^{12}CO to have a total mass of about $10^4\,\mathrm{M}_\odot$ and the component emitting ^{13}CO to have about $3 \times 10^3\,\mathrm{M}_\odot$. In addition, they identified 14 cores emitting C^{18}O. More recent extinction measurements (Lombardi & Alves 2001; Lombardi et al. 2006) increased the number of cores to more than 150 (Alves et al. 2007; Muench et al. 2007; Rathborne et al. 2009; Román-Zúñiga et al. 2010). The total mass in the upper part of the observed area ($11\,\mathrm{pc} \times 18\,\mathrm{pc}$) as inferred from extinction measurements is found to be $(11000 \pm 2600)\,\mathrm{M}_\odot$ (Lombardi et al. 2006) and thus in very good agreement with the previous CO observations[1]. It is a remarkably quiescent region and therefore often assumed to be the ideal case to study isolated star formation. Only in one tip, termed B59, observations indicate low rate star formation and probably Jeans fragmentation (Román-Zúñiga et al. 2009). The observed stars in B59 are about 2.6 Myr old (Covey et al. 2010). Recent observations with the Spitzer Space Telescope confirm the extremely low level of star formation in the Pipe Nebula (Forbrich et al. 2009). Additional observations in the near infrared (Román-Zúñiga et al. 2009, 2010), in NH3 (Rathborne et al. 2008) and X-ray (Forbrich et al. 2010) support these findings. Magnetic field observations (Alves et al. 2008; Frau et al. 2010; Franco et al. 2010) indicate that, especially in the Stem of the Pipe Nebula, the magnetic field seems to be aligned perpendicular to the main filament. Very recent observations with Herschel (Peretto et al. 2012) show that in the Stem the sub-filaments are more grid-like, whereas in B59 they are more centrally condensed.

The Pipe Nebula is located at the edge of the Sco OB2 association. The closest massive star is the B2 IV β Cephei star θ Ophiuchi (HD 157056) at a projected distance of about 3 pc from the Pipe Nebula. While its variability was known for a long time, only recently it has been target of detailed asteroseismologic studies. Non-rigid rotation was proven from multiplet observation. Observations and models (e.g. Handler et al. 2005; Briquet et al. 2007) show that θ Oph is a triple system with an inner binary. Stellar models (Lovekin & Goupil 2010) indicate that the brightest star θ Oph A can be best fit by stellar models with a luminosity of $log(L/L^C) = 3.75$ and an effective temperature $T_{\mathrm{eff}} = 22590\,\mathrm{K}$ at an age $t_{\mathrm{star}} = 15.6\,\mathrm{Myr}$. The second closest massive star is the B0 star τ Sco at a projected distance of about 20 pc.

Various models have been proposed to explain the formation and especially the observed core mass function in the Pipe Nebula (e.g. Heitsch et al. 2009). The effect of θ Oph in triggering star formation has been previously studied by Onishi et al. (1999). Here, they show that the stellar winds can not trigger star formation. However, they did not investigate the effect of the ionizing radiation in the formation and the current state of the region. In this work, we interpret the Pipe Nebula as a swept up HII-region shell. In §2 we review the underlying physics. In §3 we present analytic models and assess the current state in §4. We investigate the future evolution in §5 and conclude in §6.

2. BASIC EQUATIONS

In general, the evolution of an ionized region can be characterized by two phases. First, the ionization of the so called Stroemgren sphere (Strömgren 1939), the vol-

[1] Denote that Onishi et al. (1999) assumed a larger distance for the Pipe Nebula. The mass estimate of Lombardi et al. (2006) would be $\approx 1.7 \times 10^4\,\mathrm{M}_\odot$ at that distance.

ume which can be immediately ionized by the star before the system can react to the increased temperature and pressure. This sphere has the radius

$$R_{\rm S} = \left(\frac{3 J_{\rm Ly}}{4\pi n_0^2 \alpha_{\rm B}} \right)^{1/3}, \quad (1)$$

where $J_{\rm Ly}$ is the total ionizing flux of the source, n_0 the number density in the surrounding and $\alpha_{\rm B}$ the sum of the recombination coefficients for all levels besides the ground stage. In the second phase, the heated gas reacts to its increase in temperature and therefore pressure. An approximately isothermal shock is driven into the surrounding medium. Under the assumption of a thin shock, the time evolution of the radius is given as

$$R(t) = R_{\rm s} \left(1 + \frac{7}{4} \frac{a_{\rm s,hot}}{R_{\rm s}} (t - t_0) \right)^{\frac{4}{7}}, \quad (2)$$

where $a_{\rm s,hot}$ is the sound speed of the hot, ionized gas. The time evolution of the density in the ionized region is then given by

$$\rho(t) = \rho_0 \left(1 + \frac{7}{4} \frac{a_{\rm s,hot}}{R_{\rm s}} (t - t_0) \right)^{-\frac{6}{7}}. \quad (3)$$

For the accumulated mass we assume that the shell contains all material swept up from the HII-region, weighted by the current covering fraction f of the Pipe Nebula for the maximum size of the bubble:

$$M(t) = \frac{4\pi}{3} R(t) (\rho_0 - \rho(t)) f, \quad (4)$$

where

$$f = \frac{A_{\rm Pipe}}{4\pi R_{\rm max}^2}. \quad (5)$$

Here, $A_{\rm Pipe}$ is the current area of the Pipe Nebular tangential to the massive star and $R_{\rm max}$ is maximal radius of the HII-region, i.e. the current distance between the star and the nebula.

A more detailed treatment has to include the fact that the region around θ Oph is not spherically symmetric. Krumholz & Matzner (2009) derived an analytic approximation for blister-type HII regions. In this case

$$R_{\rm b}(t) = R_{\rm s} \left(\frac{7t}{\sqrt{6} t_{\rm s}} \right)^{\frac{4}{7}}, \quad (6)$$

where $ts = Rs/a_{\rm s,hot}$, and

$$\rho_{\rm b}(t) = \rho_0 \left(\frac{7t}{\sqrt{6} t_{\rm s}} \right)^{-\frac{6}{7}}. \quad (7)$$

$M_{\rm b}(t)$ can then be calculated according to Eq. 4.

3. FORMATION OF THE PIPE NEBULA

Using these basic equations we can now derive a model for the Pipe Nebula. In the NICER extinction maps (Fig. 1, Lombardi et al. 2006; Lada et al. 2008), a suggestive geometry can already be seen. The region around θ Oph (denoted by the asterisk) provides significantly less extinction, i.e. is less dense. We interpret this as the HII region.

In the following, we assume the cold gas to be at $T_{\rm cold} = 10\,{\rm K}$ with a mean molecular weight of $\mu_{\rm cold} = 1.37$ (Lombardi et al. 2006), corresponding to a sound speed of $a_{\rm s,cold} = 0.25\,{\rm km\,s^{-1}}$. [2] The temperature in the HII-region is resulting from the balance of heating by photoelectrons and cooling by forbidden metal lines (e.g. Osterbrock 1989).

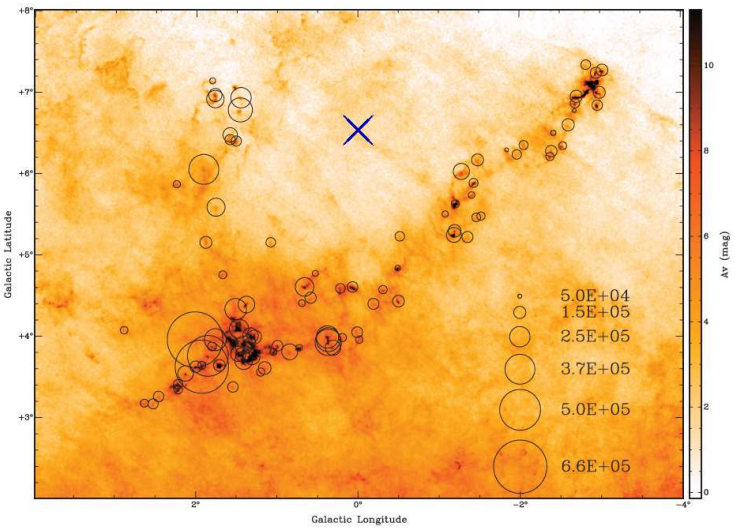

FIG. 1.— Observation of the Pipe Nebula by Lombardi et al. (2006), Figure 8 of Lada et al. (2008). The location of θ Oph is indicated by the asterisk. The size of the circles indicates the pressure of the cores (in $\rm K\,cm^{-3}$).

We test three models A, B and C, corresponding to initial number densities n_0 in the cold surrounding of $1 \times 10^3\,{\rm cm^{-3}}$, $5 \times 10^3\,{\rm cm^{-3}}$ and $1 \times 10^4\,{\rm cm^{-3}}$, respectively. In order to get a precise estimate for the radius and temperature of the initial Stroemgren sphere, we employ the radiative transfer code Cloudy. Calculations were performed with version 08.00 of Cloudy, last described by Ferland et al. (1998). We only consider the most luminous star, θ Oph A, as it is at least an order of magnitude brighter than its companions (Handler et al. 2005)[3]. We parametrize θ Oph A as a black body with a temperature of $T_{\rm eff} = 22590\,{\rm K}$ and a luminosity of $\log(L/L_\odot) = 3.75$ (Lovekin & Goupil 2010)[4]. The code Cloudy yields $R_{\rm S} = 0.094\,{\rm pc}$, $T_{\rm hot} \simeq 6000\,{\rm K}$ in case A, $R_{\rm S} = 0.029\,{\rm pc}$, $T_{\rm hot} \simeq 7000\,{\rm K}$ in case B and $R_{\rm S} = 0.017\,{\rm pc}$, $T_{\rm hot} \simeq 7000\,{\rm K}$ in case C. The corresponding sound speeds are calculated assuming a molecular weight of $\mu_{\rm hot} = 0.55$.

In Fig. 2 we show the evolution in all three cases according to Eqn. 2, 3, 6 and 7. Solid lines correspond to the classical (spherical) HII region, dashed lines correspond to the blister case. The dotted horizontal line is the value inferred from observations. It can be directly seen that in all models the final radius is bigger than 3 pc. This is especially true for the blister case. However, recent numerical simulations by Gendelev & Krumholz (2012) show that in the blister case the analytical ap-

[2] Arguably, the gas could be initially molecular, e.g. $\mu_{\rm cold} = 2.35$. As this just corresponds to a different choice of initial n_0, we assume it to be atomic to enable an easier comparison with the photo-dissociated post-shock region later on.

[3] We also neglect the influence of the B0 star τ Sco, since its projected distance to the Pipe Nebula is $\approx 20\,{\rm pc}$

[4] The simulations are performed under the assumption of a constant density, solar metallicity and a magnetic field of $B = 10^{-5}$G

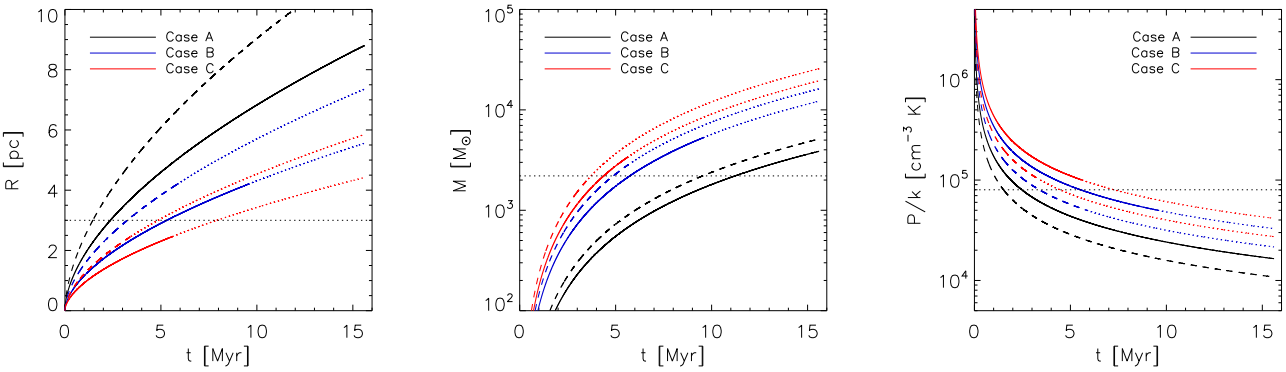

FIG. 2.— Time evolution of the HII-region for the three different cases. Solid lines: classical (spherical) HII-region, dashed: blister-type HII-region. The lines are continued dotted once the shock has reached equilibrium with the ambient surrounding. Dotted horizontal lines: current day observational values. Left panel: radius of the shell. Center: swept up mass in a Pipe Nebula sized region. Right: pressure in the hot, ionized gas.

proximation overestimates the radius. In their simulations it is only bigger by about 15% than the spherical estimate, while the analytic prediction would be 20%. In both cases the value is of order of the observed value and at the distance of the Pipe Nebula ($\approx 130 - 146\,\mathrm{pc}$) the discrepancy can be a projection effect, as Eqn. 2 and 6 give the real radius, while we can only observe the projected radius.

Next, we take a look at the mass in the swept-up shell. We estimate the surface of the Pipe Nebula tangential to the direction of the star to be the same as the projected size of the Nebula, i.e. $A_{\mathrm{Pipe}} = 14\,\mathrm{pc} \times 3\,\mathrm{pc}$. This is of course ad hoc and only an order of magnitude estimate. However, panel 2 of Fig. 2 shows clearly that in the HII-region scenario it is no problem to accumulate enough mass to be consistent with the observed value in the Pipe Nebula ($M \approx 2.2 \times 10^3\,\mathrm{M}_\odot$, see §4).

Another constraint for the models is the pressure required to confine the observed cores. Lada et al. (2008) estimate the required average pressure at the surface of the cores to be $\approx 8 \times 10^4\,\mathrm{K\,cm^{-3}}$. In our model, this pressure has to be initially supplied by the ionized gas (for a detailed discussion see §4). From Fig. 2 it can be seen that it is challenging to maintain this pressure in our model for the entire time-span of 15.6 Myr. Nevertheless, the analytical value is close to the observed value in all three cases. In addition, a closer investigation of Fig. 1 shows, that the cores in the swept up shell have lower pressures, whereas the cores in the central region have higher pressure. We discuss this further in §4.

The shock front will stagnate as soon as the pressure in the neutral gas equals the pressure in the ionized gas. This is reached in Cases B and C. Once the front stagnates, the corresponding lines in Fig. 2 are continued dotted. All three quantities are remarkably close to the observations at this point. This leads to a straightforward interpretation. The HII region expanded until stagnation. At the same time, part of the shocked gas and the post-shock gas expand, as they are preheated by the photodissociating photons of the B-star to about 100 K (see 4). The increased motion ($a_{\mathrm{s,warm}} = 0.78\,\mathrm{km\,s^{-1}}$) leads to a pile-up of material towards the solid boundary of the ionized gas and to a broadening of the shock in the opposite direction. Thus, the shock broadens with half $a_{\mathrm{s,warm}}$, reaching about 3.2 pc in the 8 Myr since stagnation in Case B. The density at stagnation in the cold shock is n_0 and will drop according to the increase in temperature. In case B, with a new temperature of 100 K, this corresponds to $500\,\mathrm{cm^{-3}}$. Taking into account the additional pile up this is very close to the value inferred from the observations ($n_{\mathrm{atomic}} = 774\,\mathrm{cm^{-3}}$, see below).

In addition, the equations in §2 are derived under the approximation of a thin shock. This approximation will fail eventually. Then, the speed of the ionization front will be lower than the analytical estimate. Therefore, the radius and swept up mass are best viewed as an upper limit. Correspondingly, the pressure is a lower limit, since a smaller region will lead to higher densities and thus to a higher pressure in the ionized gas.

4. CURRENT STATE

We now continue to discuss the current state of the Pipe Nebula in more detail. The most obvious constraints are the mass, pressure and current size.

To asses the current mass, it is necessary to take a detailed look at the observations. The total mass in the upper part of the observed region ($b > +3°$) is inferred to be $10^4\,\mathrm{M}_\odot$ from extinction measurements by Lombardi et al. (2006). They provide a detailed comparison with the previous ^{12}CO-measurements by Onishi et al. (1999) and find encouraging agreement. To estimate the mass inside the Pipe Nebula itself it is first necessary to look at the mass in the dense component alone. From Lombardi et al. (2006) Fig. 7, it is reasonable to assume that the dense component has an extinction $A_K > 0.4$. Inside this isoextinction contour there is about 40% of the total mass (Lombardi et al. 2006, their Fig. 27). About half of this mass is in the Pipe Nebula, therefore the denser component of the nebula itself has a mass of about $2.2 \times 10^3\,\mathrm{M}_\odot$. This is in agreement with the $3 \times 10^3\,\mathrm{M}_\odot$ in the entire region inferred by Onishi et al. (1999) from ^{13}CO, which traces the denser gas (e.g. their Fig. 5). The total mass in the cores is about $250\,\mathrm{M}_\odot$ (Lada et al. 2008, their Table 1).

From these masses, we can derive the structure of the Nebula. The cores have a known pressure of $\approx 8 \times 10^4\,\mathrm{K\,cm^{-3}}$. The ionized gas can supply this pressure. Independent of the uncertainties in §3, we perform a Cloudy simulation on the current static state. It

shows, that θ Oph A can ionize gas at $n_0 = 8\,\mathrm{cm}^{-3}$ up to a radius of 2.75 pc to $T = 5000\,\mathrm{K}$. With $\mu_{\mathrm{ion}} = 0.55$ the pressure is then $7.3 \times 10^4\,\mathrm{K\,cm}^{-3}$, which is a bit less than the observed average density of the cores. However, a closer look at Fig. 1 reveals, that the cores along the rim generally have a lower pressure (i.e. smaller circles), whereas the high pressure cores are towards the central region. A straightforward assumption is that the atomic component in between the cores and the ionized gas is in pressure equilibrium with both, acting as a buffer. Assuming a volume of $14\,\mathrm{pc}\times3\,\mathrm{pc}\times2\,\mathrm{pc}$ for the Pipe Nebula, and $\mu = 1.37$ (Lombardi et al. 2006), this corresponds to $n_{\mathrm{atomic}} = 774\,\mathrm{cm}^{-3}$. To be in pressure equilibrium, the atomic phase has to be at $T = 100K$. Thus, the bulk of the mass ($\approx 87.5\%$) is in the atomic phase. To keep the medium at this temperature, significant heating is required. The heating can be supplied by the diffuse radiation. In addition, Arthur et al. (2011) showed that for B-stars the photo-dissociation-region (PDR) is wider than for O-stars. This is due to the peak at lower energies in the spectrum. Therefore, in B-stars, the ratio of photo-dissociating photons to ionizing photons is higher. As a consequence, the photo-dissociation, i.e. the disruption of H_2 molecules, outruns the ionization front, leading to a warmer region at about 100 K with a thickness of about 30% of the radius of the HII region.

Concerning the high pressure cores in the central region, it is probably best to assume that this region is currently undergoing gravitational collapse. Possibly, the swept up HII-shell encountered a denser region and the resulting density enhancement lead to a gravitational unstable region. Thus, the cores in the region are gravitationally bound.

The width of the Pipe Nebula can be explained by assuming the shock and post-shock region expand after stagnation with $\frac{1}{2}a_{\mathrm{s,warm}}$ (see §3). Therefore, the Case C would lead to 4.4 pc and Case B to 3.2 pc, as observed.

5. FURTHER EVOLUTION AND IMPLICATIONS FOR THE IMF

As the bulk of the mass is in the atomic phase, this phase will most likely determine the future evolution of the Pipe Nebula. A possible scenario is triggered star formation from within. When the most massive clumps turn into stars, they will ionize and thereby heat the atomic phase. This will in turn increase the pressure on the cold cores, forcing them to form stars.

In the context of the transition from the Core Mass Function (CMF) to the Initial Mass Function (IMF) it is very interesting to look at the increase of the ambient pressure quantitatively. If the radiation of the newborn stars increases the background pressure by a factor of two, the shift from the IMF to the CMF could be explained (Lada et al. 2008).

There are three cores of about $10\,\mathrm{M}_\odot$ and one with $\approx 20\,\mathrm{M}_\odot$ in the Pipe Nebula. Assuming that the entire most massive cores end up in a single stars, the further evolution will be similar to our model A. As can be directly seen from Fig. 2, there would be a shock proceeding through the Pipe nebula. However, due to the number density in the atomic gas, the evolution of this shock would take several Myr, whereas star formation in general seems to be more synchronized. For the $10\,\mathrm{M}_\odot$ cores, the evolution would be even slower. Furthermore, this triggering scenario would leave the top end of the IMF unaffected as these cores turn into stars before they themselves increase the ambient pressure.

A more violent scenario will occur if θ Oph explodes in a supernova before the massive cores turn into stars. Given the relatively small distance, the Pipe Nebula will be hit by a blast wave in the Sedov phase within a few kyr after the explosion. Mostly likely, the smaller cores will get disrupted, while the bigger cores will get triggered into collapse within another few kyr (see e.g. Gritschneder et al. 2012). This could indeed explain the small age spread observed in star forming regions.

Another environmental effect is the influence of the Sco OB2 association. As pointed out previously (e.g. de Geus 1992) and discussed recently by Peretto et al. (2012), the star forming region termed B59 is pointing towards that association and resembles a bow shock like structure. However, the age estimate for the young stars in B59 of 2.6 Myr (Covey et al. 2010) suggests that this interaction triggered the stars in the past and is not currently driving star formation further down the stem.

6. DISCUSSION & CONCLUSIONS

There are several uncertainties involved in the model. The main uncertainty lies in the assumption of a thin shock for the analytic solution. Once the shock thickens, it will lead to a smaller region and a less dense shell with a higher pressure, as discussed above. Another possibility to constrain the HII region to the current size would be magnetic fields. Krumholz et al. (2007) were able to demonstrate that the evolution of a shell stagnates earlier for a magnetized medium since the Alfven speed is higher than the sound speed (see also Arthur et al. 2011).

Another uncertainty lies in the assumed initial conditions for the Cloudy models, e.g. the assumed abundances, grains and magnetic fields will influence the outcome. However, for the temperature and the size of the HII region, these simulations give more realistic answers than the simple assumptions leading to Eq. 2. Furthermore, the most important input parameter - besides the stellar parameters taken directly from observations - is still the density, as it enters with n_0^2.

The assumed time scale for the sweeping up of the Pipe Nebula is ≈ 15 Myr. This is comparable to the free-fall time of a cloud so a remaining question is why the nebula did not collapse. One possible solution might be the finding of Arthur et al. (2011) that B-stars have an extended PDR. In this broad region behind the ionization front the temperature is close to 100K. As e.g. shown by Gritschneder et al. (2010), a higher temperature in the cold gas is prohibitive of structure formation and thus hindering collapse.

Besides these uncertainties, the scenario of θ Oph swiping up the Pipe Nebula presented in this paper can, especially in Case B, successfully explain:

1. The observed morphology of the Pipe Nebula, especially the spheroidal shape of the less dense region.

2. The current width, as a shock broadening with $\frac{1}{2}a_{\mathrm{s,warm}} = 0.44\,\mathrm{km\,s}^{-1}$ will reach a width of 3.2 pc in the 8 Myr since the stagnation.

3. The current mass and size can be easily reached.

4. More importantly, the pressure to confine the cores can be supplied.

Especially the pressure of the cores is otherwise puzzling. Up to now, the only possible explanation for this confinement was the self-gravity of the cloud. This is highly unlikely, as the cores in a self-gravitating system are the first instances to react to the collapse and therefore should be bound, whereas most of the cores are observed to be unbound.

7. ACKNOWLEDGEMENTS

M.G. acknowledges funding by the Alexander von Humboldt Foundation in form of a Feodor-Lynen Fellowship and by the China National Postdoc Fund Grant No. 20100470108 and the National Science Foundation of China Grant No. 11003001. D.N.C.L. acknowledges funding by the NASA grant NNX08AL41G.

REFERENCES

Alves, F. O., & Franco, G. A. P. 2007, A&A, 470, 597
Alves, F. O., Franco, G. A. P., & Girart, J. M. 2008, A&A, 486, L13
Alves, J., Lombardi, M., & Lada, C. J. 2007, A&A, 462, L17
Arthur, S. J., Henney, W. J., Mellema, G., de Colle, F., & Vázquez-Semadeni, E. 2011, MNRAS, 414, 1747
Briquet, M., Morel, T., Thoul, A., Scuflaire, R., Miglio, A., Montalbán, J., Dupret, M.-A., & Aerts, C. 2007, MNRAS, 381, 1482
Covey, K. R., Lada, C. J., Román-Zúñiga, C., Muench, A. A., Forbrich, J., & Ascenso, J. 2010, ApJ, 722, 971
de Geus, E. J. 1992, A&A, 262, 258
Ferland, G. J., Korista, K. T., Verner, D. A., Ferguson, J. W., Kingdon, J. B., & Verner, E. M. 1998, PASP, 110, 761
Forbrich, J., Lada, C. J., Muench, A. A., Alves, J., & Lombardi, M. 2009, ApJ, 704, 292
Forbrich, J., Posselt, B., Covey, K. R., & Lada, C. J. 2010, ApJ, 719, 691
Franco, G. A. P., Alves, F. O., & Girart, J. M. 2010, ApJ, 723, 146
Frau, P. et al. 2010, ApJ, 723, 1665
Gendelev, L., & Krumholz, M. R. 2012, ApJ, 745, 158
Gritschneder, M., Burkert, A., Naab, T., & Walch, S. 2010, ApJ, 723, 971
Gritschneder, M., Lin, D. N. C., Murray, S. D., Yin, Q.-Z., & Gong, M.-N. 2012, ApJ, 745, 22
Handler, G., Shobbrook, R. R., & Mokgwetsi, T. 2005, MNRAS, 362, 612
Heitsch, F., Ballesteros-Paredes, J., & Hartmann, L. 2009, ApJ, 704, 1735
Krumholz, M. R., & Matzner, C. D. 2009, ApJ, 703, 1352
Krumholz, M. R., Stone, J. M., & Gardiner, T. A. 2007, ApJ, 671, 518
Lada, C. J., Muench, A. A., Rathborne, J., Alves, J. F., & Lombardi, M. 2008, ApJ, 672, 410
Lombardi, M., & Alves, J. 2001, A&A, 377, 1023
Lombardi, M., Alves, J., & Lada, C. J. 2006, A&A, 454, 781
Lovekin, C. C., & Goupil, M.-J. 2010, A&A, 515, A58
Muench, A. A., Lada, C. J., Rathborne, J. M., Alves, J. F., & Lombardi, M. 2007, ApJ, 671, 1820
Onishi, T. et al. 1999, PASJ, 51, 871
Osterbrock, D. E. 1989, Astrophysics of gaseous nebulae and active galactic nuclei (University Science Books)
Peretto, N. et al. 2012, A&A, 541, A63
Rathborne, J. M., Lada, C. J., Muench, A. A., Alves, J. F., Kainulainen, J., & Lombardi, M. 2009, ApJ, 699, 742
Rathborne, J. M., Lada, C. J., Muench, A. A., Alves, J. F., & Lombardi, M. 2008, ApJS, 174, 396
Román-Zúñiga, C. G., Alves, J. F., Lada, C. J., & Lombardi, M. 2010, ApJ, 725, 2232
Román-Zúñiga, C. G., Lada, C. J., & Alves, J. F. 2009, ApJ, 704, 183
Strömgren, B. 1939, ApJ, 89, 526